Available online at www.sciencedirect.com

SciVerse ScienceDirect

Physics Procedia 37 (2012) 1171 – 1178

Physics Procedia

# TIPP 2011 - Technology and Instrumentation for Particle Physics 2011

# Time Calibration of the ANTARES Neutrino Telescope

Umberto Emanuele on behalf of the ANTARES Collaboration

*IFIC - CSIC - Edificio Institutos de Investigacin. Paterna. Valencia. E-46071 Spain*

**Abstract**

The ANTARES deep-sea neutrino telescope consists of a three dimensional array of photomultipliers to detect the Cherenkov light induced by relativistic charged particles originating from neutrino interactions in the vicinity of the detector. It was completed in 2008 and is taking data smoothly since then. The large scattering length of light in the deep sea allows for an angular resolution of a few tenths of a degree for neutrino energies exceeding 10 TeV. In order to achieve this optimal performance, the time calibration systems should ensure a measurement of the relative time offsets between the photomultipliers at the level of about 1 ns. The time calibration is performed through different systems/procedures: the on-shore calibration in a dark room, the echo-based clock system, the internal LEDs, the Optical Beacon systems and the potassium-40 present in the water. In this contribution, the methods developed to attain the needed level of precision and the results obtained with the data taken *in situ* will be shown.



*Keywords:* Time calibration, Neutrino Telescopes, ANTARES

## 1. Introduction

The ANTARES neutrino telescope has been constructed in the Mediterranean Sea [1], with the main purpose of the search for high-energy neutrinos of astrophysical origin. The detection principle is based on the tracking down of Cherenkov photons induced by the passage of relativistic charged particles resulting from neutrino interactions in the material surrounding the detector, the most important channel being the charged current interactions producing muons. The angular resolution of the track reconstruction depends on the accurate measurement of the arrival time of Cherenkov photons reaching the photon sensors. Water-based neutrino telescopes have as intrinsic and unavoidable limitations in the time precision: the chromatic dispersion and scattering of light in water ($\sigma \sim 2$ ns for a traveling distance of 50 m) and the combined effect of the photomultiplier transit time spread and electronics ($\sigma \sim 1.5$ ns). Taking into account these intrinsic limitations, the required precision of a time calibration system to measure the relative time between photo-sensors should be $\sigma \leq 1$ ns. The absolute time calibration is less demanding. A precision of a few seconds is sufficient to correlate reconstructed neutrino directions with steady point sources and an accuracy of the order of milliseconds is sufficient for association to transient astrophysical events (GRBs, AGN flares, SGR bursts, etc.) As it will be explained later, the GPS system provides a good enough time stamping.

[1]Corresponding author's email address: *emanuele@ific.uv.es*

1875-3892 © 2012 Published by Elsevier B.V. Selection and/or peer review under responsibility of the organizing committee for TIPP 11. Open access under CC BY-NC-ND license. doi:10.1016/j.phpro.2012.02.456

[a] 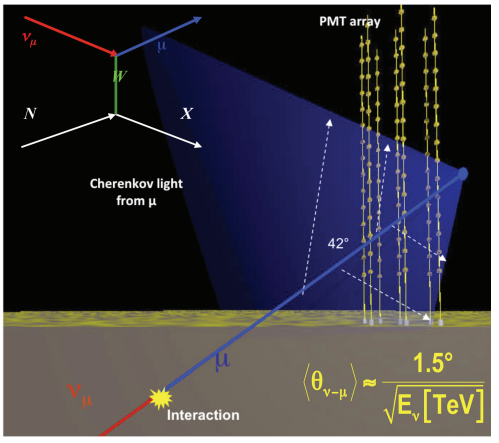

[b] 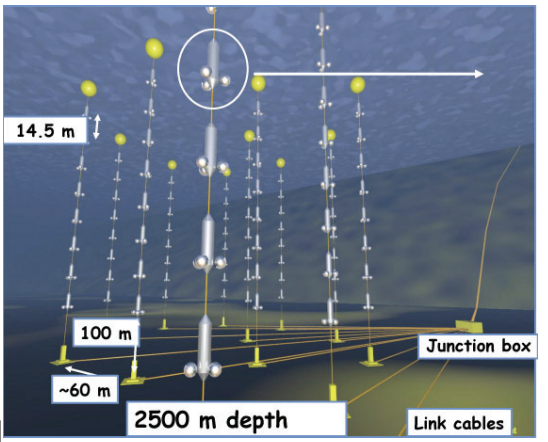


Figure 1: a) Detection principle of the Cherenkov light from a muon. b) ANTARES detector layout.

## 2. The ANTARES neutrino telescope

The ANTARES detector is located in the Mediterranean Sea, about 40 km from Toulon, off the French coast. It consists of 885 10−inch PMTs (model R7081-20 from Hamamatsu) distributed over twelve lines, in 25 triplet-PMT storeys each and anchored to the sea bottom. The total length of each line is 480 m. The lowest storey of each line is located 100 m above the sea bed. The distance between consecutive storeys is 14.5 m and the horizontal separation between lines is 60−80 m.

The PMTs [2] are coupled with optical gel to the inner surface of pressure−resistant glass spheres (optical modules, OMs [3]). A $\mu$−metal cage inside the OM shields the PMT from the Earth magnetic field. Each storey comprises a triplet of OMs and a titanium container with all the electronics of the storey (Local Control Module, LCM). Five consecutive storeys along the line are grouped into a sector sharing common data and clock distribution elements. One LCM of a sector (Master Local Control Module, MLCM) allows data connection from all sectors of the line to shore along optical fibers. At the bottom of each line, a String Control Module (SCM) houses the power units. Furthermore, each line incorporates four LED Optical Beacons (OBs) [4] used for time calibration and studies of the optical properties of the sea water; and two Laser Beacons are located at the bottom of two of the central lines. The lines are connected to a junction box (JB) from where the Main Electro−Optical Cable (MEOC), of a length of 45 km, links the detector to the shore station. The shore station houses a computer farm for data filtering and storage and the master clock. A more detailed description of the ANTARES DAQ system can be found in [5]. The signals from one PMT are processed *in situ* by ASICs (named Analogue Ring Samplers or ARSs [6]), located in the LCMs. Two ARSs are used in alternation on each OM in order to reduce the dead time of the PMT signals close in time. The clock period of 50 ns covers about 150 channels of the ADC, corresponding to an average bin width of 0.3 ns. The resulting effective time resolution, including non-linearities of the ADCs, results adequate for the requirement of a time resolution below 1 ns. Using a fixed amplitude threshold in order to discriminate the PMT signals by the ARSs, could introduce a particular effect; for instance PMT signals with high amplitude cross the threshold earlier than coincident low amplitude signals: this effect is called: ”walk effect”. The knowledge of the photo-electron pulse shape (PPS) can be used to correct this effect: the PPS function is scaled up or down to reproduce the total charge of the hit and the corresponding threshold − crossing time is calculated. The walk effect correction is strictly applied in event reconstruction.

## 3. The Clock System

In order to synchronize the readout of the whole detector, a clock signal is generated to provide a common signal for all the OMs. It consists of a 20 MHz generator on shore, whose signal is distributed into a network, ending in each LCM with a transceiver.

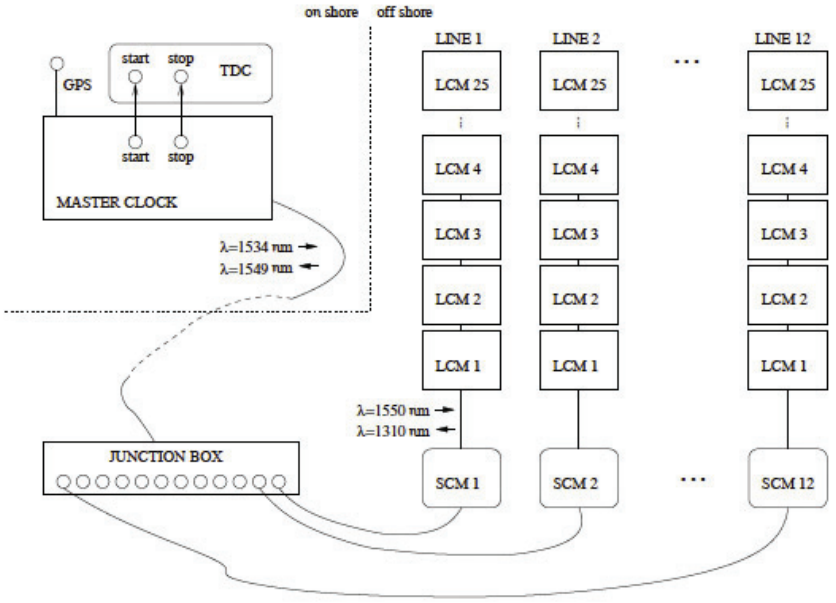


Figure 2: **Clock system main scheme.**

The absolute time stamping is performed by interfacing the clock system with a dedicated electronic board to the GPS timing system that provides a time accuracy of ∼100 ns with respect to the Universal Time Coordinated. The angular resolution of the track reconstruction depends on the accurate measurement of the arrival time of Cherenkov photons reaching the photon sensors. The clock distribution network, shown in Figure 2, is based on a bidirectional optical communication system that allows communication between shore and the SCMs of the lines. Although the clock system provides a common signal, special clock signals are addressed to each LCM clock transceiver in order to measure the time delays for individual storeys due to the propagation time along the cables. The corresponding round-trip time is twice the propagation time to each individual LCM. During the standard operation of the telescope, the round-trip times to all the LCMs of the detector are monitored once per hour, which ensures having at least one measurement per data taking run. An average of many such measurements provides the required precision.

## 4. Time Calibration system and methods

The time slot between the incidence of a photon on the PMT photocathode and the time stamping of the associated signal in the ARS must be determined. This is strongly dependent on the ARS threshold, the front-end electronics response time, the PMT signal transit time and the length of the cable linking the OM to the LCM. The intrinsic time offsets of the system are determined in a first step by means of a dedicated calibration set-up in a dark room, prior to deployment. These constants could change slightly after deployment due to the temperature changes, stressing of cables during transportation/deployment, etc. Moreover the variation of the high voltage applied to the PMTs, could cause modifications in these time offsets. Using the optical beacon system, they are periodically monitored and recomputed when the lines are operated in the sea.

### *4.1. Onshore calibration*

As mentioned, in a first step, the functionality of each line is verified and a complete calibration is performed before deployment. The onshore time calibration is carried out illuminating simultaneously groups of OMs by short laser pulses. The propagation times from SCM to LCM are known from the clock system calibration, so the contribution from the linking cable, the PMT transit time and the front-end electronics delay can thus be extracted.

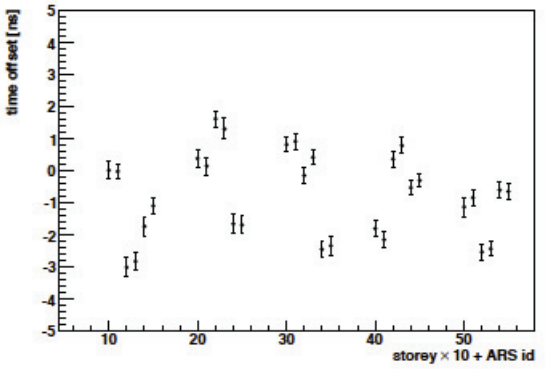


Figure 3: **Time offsets measured for all ARSs of one of the line sectors. The time offsets are relative to the first ARS of the first OM of the lowest storey. The ARS id runs from 0 to 5 within each storey.**

The time calibration is performed per sector (5 storeys) in the dark room. The light source used is a Q-switched, Nd-YAG laser that emits intense (E ∼1 $\mu$J) and short (FWHM ∼ 0.8 ns) pulses of green light ($\lambda$=532 nm) externally triggered at a frequency of 1 kHz. The light is distributed to the 15 OMs of each sector through optical fibers, previously splitted. Each optical fibre is coupled to a Lambertian diffuser which spreads the laser light over the full area of the corresponding PMT photocathode. The output amplitude of the light (equivalent to about $10^{12}$ photons) is attenuated in order to produce a few tens of photoelectrons in the PMTs.

An example of the distribution of the difference between the time of the signal recorded by an OM and the emission time of the pulse as recorded by the laser photodiode (used to establish the time stamp of the signal) is shown in Figure 3. The mean value of this distribution yields the difference between the laser light signal time measured by the PMT (including the PMT transit time and the electronics delay) and the time measured by the photodiode channel. The sigma of the distribution is 0.5 ns. The time offsets between each OM of a line and the first OM of its lowest storey, which is chosen as a reference, are computed for each of the 30 ARSs of each sector. The relative time calibration of the monitoring PMTs of the LED optical beacons (used for the *in situ* calibration described in subsection 4.2.1) is also performed during the onshore calibration. One of the fibers of the optical splitter is used in this case to send the light to the small PMT within each OB. Since this PMT is meant to measure the relatively high intensity of light emitted by the LEDs, the incident laser light intensity is tuned to be about twenty times higher than that provided to the OMs.

### *4.2. In situ calibration:* the optical system

Once the detector is deployed, the *in situ* measurement of the time offsets of the OMs is performed by means of the optical beacon system [3]. This consists of two different devices: LED beacons, that emit with $\lambda$ = 470 nm (blue light), and laser beacons emitting with $\lambda$ = 532 nm (green light) . The two kinds of devices are used to perform different calibrations: intra-line and inter-line. In particular the LED beacons represent a fundamental monitor for relative time offsets between OMs of the same line measurements, whereas the laser beacons are used for monitoring the relative time offsets between the lines, and the calibration of the lowest storeys. The *in situ* calibration allows to correct the time constants computed onshore, fixing the offset changes due to different factors, particularly in case of changes in the PMT high-voltage and threshold settings.

#### *4.2.1. LED beacons*

Along every line of the detector (in storeys 2, 9, 15 and 21), four LED optical beacons are distributed. Each LED OB contains 36 LEDs distributed on six faces forming a hexagonal prism. The LEDs emit blue light with a maximum intensity of ∼160 pJ per flash (∼4 x $10^8$ photons per pulse) and a pulse width of 4 ns (FWHM). A special PMT (8-mm) placed inside the frame of the LED OB is used to measure the emission time of the LED light. Figure 4-b) shows the distribution of signal time residuals, i.e. the difference between the signal time recorded in the OM and the emission time of the corresponding LED flash, using the time offsets measured in the dark room and once the nominal travel

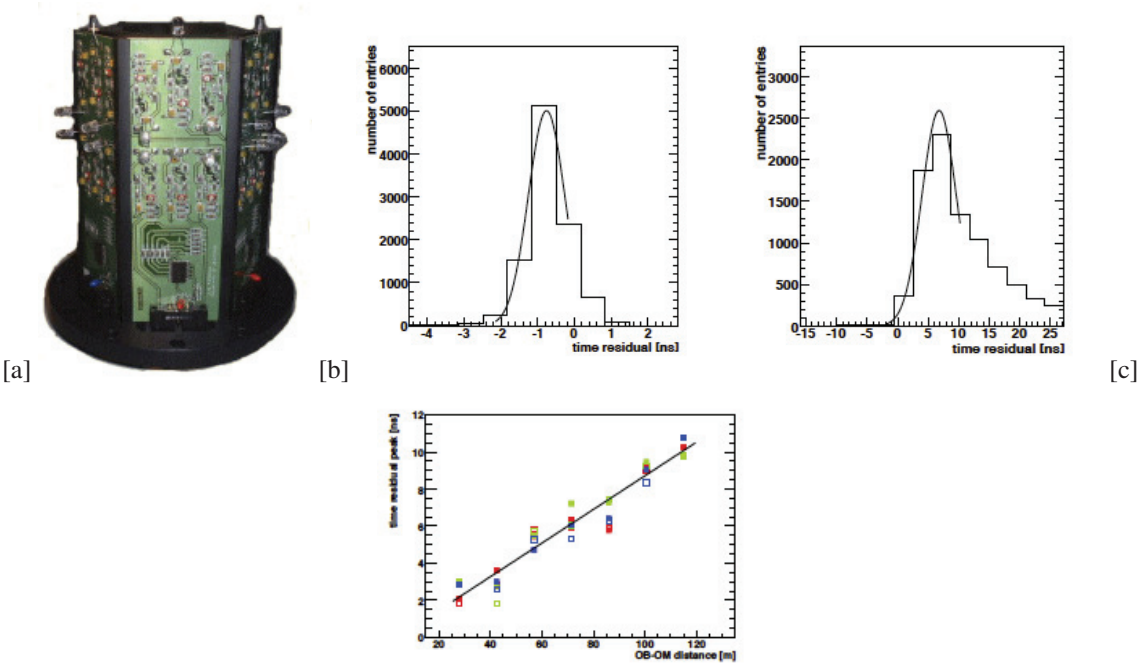


Figure 4: a) LED beacon. b) Time residual distribution in two different OMs located two storeys (left) and seven (right) above the source beacon. c) Time residual peak position as a function of the OB-OM distance.

time of the light from the beacon to the OM has been subtracted. It is possible to observe differences in the two parts of the plot: the one on the left shows the distribution corresponding to an OM close to the OB (∼30 m), which receives a high amount of light. The plot on the right shows the distribution for an OM located seven storeys above the OB (∼100 m). In this case, a tail at positive times due to light scattering in water can be observed. A Gaussian-Exponential convolution function could fit to the region including the rising edge of the time distribution and the first bin after its maximum. A method to analyze the time offsets has been optimized based on this fit. Moreover the range of the fit is restricted in order to use mostly the earliest photons, whose delay due to scattering can be neglected. An example of the position of the time residual peak as a function of the distance from the OM to one optical beacon is shown in Figure 4-c): the slopes of such fits for all the OBs are also shown in the figure.

Time residuals should be characterized by mean values well centered at zero, but in practice it's not so obvious.The increase of the time residual with distance originates from an early photon effect, arising from the duration of the light pulse and the fact that the first photons detected by the PMT determine the recorded time of the pulse [7].

The PMTs closer to the source trigger on the photons emitted earlier in the flash, whilst for PMTs farther away the probability distribution for the measured time of the signal is determined by the pulse width. The arrival time of the first photon obeys the order statistics [8]. At high regimes, a linear increase in the time residual is expected, due to the combination of different effects (early photon and exponential decreasing of the intensity caused by the light attenuation).

A straight line is fitted to the time residual peaks ordered by the distance of the optical modules from the optical beacon. If a point deviates more than 2 ns, the fit is redone excluding it. From first analysis it is found that 15% of the cases need a correction to the dark room offsets larger than 1 ns. Seven storeys above each OB, excluding the one just above the beacon (which receives too much light), can be calibrated. The storeys farther away, which do not receive enough light, are monitored with the next OB along the line. The OMs of the first three storeys of each line have to be calibrated by the laser beacon and potassium-40 [9].

*4.2.2. Laser beacon*

As already mentioned, to measure the relative time deviation between lines the laser beacons are used. The laser is much more powerful than the LED beacons, so by means of a laser beacon it is possible to illuminate almost all the detector.

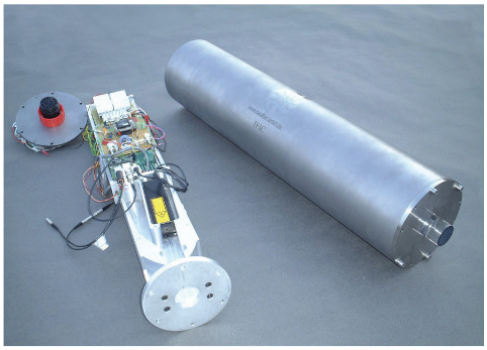

Figure 5: **Laser beacon: the internal mechanics, the connector cap and the titanium container.**

This inter-line calibration is needed because the time offsets measured in the dark room are calculated with respect to a reference OM specific to each line. It is possible to conclude that in the case of the laser, due to the very narrow (FWHM~0.8 ns) time width of the pulse and considering that only distances where the OMs are illuminated below the one-photoelectron level are considered, the early photon is negligible. For this reason, the time offsets do not depend on the distance to the source, and the relative time deviations between lines could be evaluated as the average of the time residual peaks. An example of calculated inter-line time offsets is plotted in Figure 6.

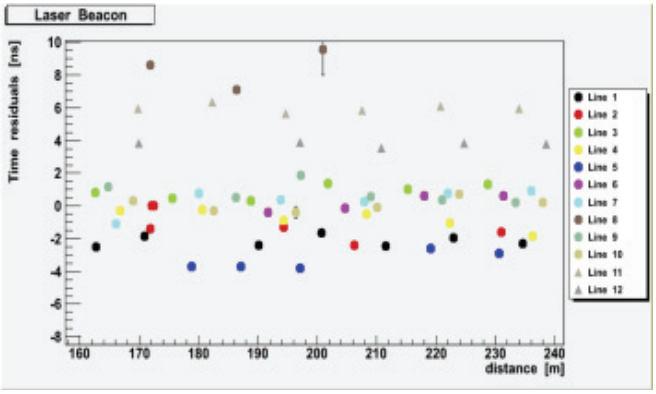


Figure 6: **Time residual peak position versus the distance between the laser beacon and the OM.**

An important additional thing is that, as commented before, the laser beacon also represents a reliable medium to compute the time offsets located the OMs in the lowest storeys, before the first LED Beacon [9].

*4.3. Potassium-40*

The radioactive potassium-40 ($^{40}K$) present in sea water can be used for time and efficiency calibration of the detector using the Cherenkov light induced by the electron emitted in the $\beta$-decay of potassium [3,9]. In case that a decay occurs at distance in a range of few meters from a storey, signals in coincidence can be detected by two OMs. A posteriori conclusion is that using the time offsets calculated *in situ* instead of the determined from the dark room calibration, the RMS of the intra-storey time difference distribution determined by this method improves from 0.72 ns to 0.57 ns. So $^{40}K$ represents a complementary and independent calibration method.

### 4.4. Internal LEDs

An internal LED is also present in each optical module, with the aim to monitor the stability of the PMT transit time. The LED is located on the back of the phototube and illuminates the photocathode from behind. The clock signal (constant rate) is used to trigger this LED.

## 5. Contribution of the front-end electronics

During the two calibration steps, onshore and *in situ*, it is needed to evaluate the influence of the front-end electronics on the time resolution. Here below three different methods to estimate the front-end electronics contribution in ANTARES are described. At low light intensity, the time resolution of an OM measured in the laboratory is dominated by the transit time spread of the PMT ($\sigma_{TTS} \sim 1.3$ ns). At high intensity, this contribution decreases as the square root of the number of photoelectrons and therefore the dominant term to the width of this distribution is the constant contribution due to the front-end electronics. In the dark room calibration this minimum contribution is found to be ∼0.5 ns.

Once deployed the detector, the time resolution of the electronics is calculated as the distribution of the time difference measured by an OM close to an OB with respect to the emission time of the OB pulse.

The sigma of the time distribution of the signal in an OM is given by the formula:

$$\sigma^2_{OM} = \frac{\sigma^2_{TTS}}{\mathrm{N}_{pe}} + \frac{\sigma^2_{water}}{N_\gamma} + \sigma^2_{OB} + \sigma^2_{elec} \tag{1}$$

where $\sigma_{TTS}$ is the transit time spread of the PMT, $\sigma_{water}$ is the spread due to the scattering and chromatic dispersion of light in water (∼1.5 ns for a light path of 40 m), $\sigma_{OB}$ is the uncertainty of the measured emission time of the pulse and $\sigma_{elec}$ the spread due to the electronics. At high regime (OM close to an OB), the values of Npe and N$\gamma$ are high, and their corresponding contributions become negligible. Due to the fast rise time of the internal PMT of the OB, $\sigma_{OB}$ can also be neglected. Taking into account many measurements at high light regime a time resolution of ∼0.5 ns for the electronics is obtained, in good agreement with the results obtained during the first calibration (onshore).

A third way to check this time resolution is given by comparing the times measured by two OMs in the same storey when illuminated at high intensity, and also in this case a time resolution of 0.5 ns is obtained. It is possible to conclude that the readout system contributions are negligible with respect to the ones from the TTS and chromatic dispersion [9].

## 6. New Laser deployment in ANTARES

At present, a Laser Beacon located at the bottom of Line 8 is working in ANTARES. Several studies have been carried out to obtain an optimized configuration of a new Laser Beacon: for instance, concerning a more powerful laser, an upgraded design of the cylinder quartz Rod and a new titanium container. Taking advantage of the recovery of the ANTARES instrumentation line during the spring of the present year, this new Laser Beacon has been integrated and developed on the bottom of the refurbished instrumentation line. The deployment of this LB not only completes the Optical Calibration System of ANTARES, but it is important for testing and developing a new calibration device for KM3NeT, which is currently in its Pre-Production Model (PPM) phase [10]. In particular, by means of this new laser, a crosscheck with the present one will be feasible, more sophisticated optical properties measurements will be performed, and a better optical time calibration will be done. On the other side, and concerning KM3NeT, the resistance of the Laser Beacon container to the pressure and the communications between the main control board and light emitting source will be tested. The reliability of the electronics in general will be checked and the light range will be measured.

## 7. Conclusions

ANTARES represents a fundamental device for the neutrino detection in the neutrino Southern sky. One of the main features of the detector is its angular resolution (a few tenths of a degree above 10 TeV). The track reconstruction algorithms are based on the PDF of the photon arrival times to the PMTs. For this reason a precise time calibration of the system is crucial to ensure an optimal functionality. As described, a preliminary time calibration is performed in the laboratory (onshore calibration). As a consequence of the movements, temperature, changes in high voltage and other factors, a *in situ* calibration, performed by a system of optical beacons, is needed. The adopted calibration systems and methods attain a relative time calibration between detector elements of less than 1 ns, as required.

The experience gained in ANTARES represents an important result, and it will be used also to design the calibration system of KM3NeT, the future cubic kilometer-scale neutrino telescope [10].

## 8. Acknowledgments

The authors acknowledge the financial support of the funding agencies: Centre National de la Recherche Scientifique (CNRS), Commissariat *à* l'*é*nergie atomique et aux energies alternatives (CEA), Agence National de la Recherche (ANR), Commission Europenne (FEDER fund and Marie Curie Program), Region Alsace (contrat CPER), Region Provence-Alpes-C*ô*te dAzur, Departement du Var and Ville de La Seyne-sur-Mer, France.

Bundesministerium f*ü*r Bildung und Forschung (BMBF), Germany; Istituto Nazionale di Fisica Nucleare (INFN), Italy; Stichting voor Fundamenteel Onderzoek der Materie (FOM), Nederlandse organisatie voor Wetenschappelijk Onderzoek (NWO), the Netherlands; Council of the President of the Russian Federation for young scientists and leading scientific schools supporting grants, Russia; National Authority for Scientific Research (ANCS), Romania; Ministerio de Ciencia e Innovacion (MICINN), Prometeo of Generalitat Valenciana (GVA) and MultiDark, Spain.

We also acknowledge the technical support of Ifremer, AIM and Foselev Marine for the sea operation and the CC-IN2P3 for the computing facilities.

## 9. References

[1] P. Coyle for the ANTARES Collaboration, The ANTARES deep-sea neutrino telescope: status and first results, Proc. of the 31st ICRC, Lodz (2009), eprint astro-ph/1002.0754

[2] J.A. Aguilar et al., ANTARES Collaboration, Study of large hemispherical photomultiplier tubes for the ANTARES neutrino telescope, Nucl. Instr. and Meth. A 555 (2005) 132-141, eprint physics/0510031

[3] P. Amram et al., ANTARES Collaboration, The ANTARES Optical Module, Nucl. Instr. and Meth. A 484 (2002) 369-383, eprint astro-ph/0112172

[4] M. Ageron et al, ANTARES Collaboration, The ANTARES Optical Beacon system, Nucl. Instr. and Meth. A 578 (2007) 498-509, eprint astro-ph/0703355

[3] J.A. Aguilar et al., ANTARES Collaboration, Study of large hemispherical photomultiplier tubes for the ANTARES neutrino telescope, Nucl. Instr. and Meth. A 555 (2005) 132-141, eprint physics/0510031

[4] P. Amram et al., ANTARES Collaboration, The ANTARES Optical Module, Nucl. Instr. and Meth. A 484 (2002) 369-383, eprint astro-ph/0112172

[5] J. A. Aguilar et al, ANTARES Collaboration, The data acquisition system for the ANTARES neutrino telescope, Nucl. Instr. and Meth. A 570 (2007) 107-116, eprint astro-ph/0610029

[6] J. A. Aguilar et al, ANTARES Collaboration, Performance of the front-end electronics of the ANTARES Neutrino Telescope, Nucl. Instr. and Meth. A (2010), doi:10.1016/j.nima.2010.06.225, eprint astro-ph/1007.2549v1

[7] J. A. Aguilar Analysis of the Optical Beacon system and search for point-like sources in the ANTARES neutrino telescope, Ph.D thesis, Univ. of Valencia (2007), http://antares.in2p3.fr/Publications

[8] M. Kendall and A. Stuart, The advanced theory of Statistics I, Ed. Oxford University Press, ISBN 0852642857

[9] J.A. Aguilar et al. ANTARES Collaboration, "Time Calibration of the ANTARES Neutrino Telescope", Astropart.Phys.34:539-549, 2011

[10] U. Emanuele et al. KM3NeT Consortium, "Time Calibration of the KM3NeT Neutrino Telescope", TIPP2011 Physics Procedia Proceedings, 2011